HEAT TRANSFER COEFFICIENT DURING WATER JET COOLING OF HIGH-TEMPERATURE STEEL*

Hormando Leocadio[1]
CWM van der Geld[2]
Julio Cesar Passos[3]

Abstract
Impinging water jets promote high heat flux extraction rate. Steel industry widely employs the process for accurate temperature control to improve the microstructure and to ensure adequate mechanical properties. The range of surface temperatures, heat fluxes and cooling rates are very large, which makes it important to obtain an accurate value of the heat transfer coefficient. This paper presents an experimental and numerical study of the heat transfer behavior of a high temperature (450°C - 900°C) steel plate cooled by a water jet at 20°C to 70°C. High-speed imaging (up to 20,000 fps) within water jet impingement zone allowed the characterization of the boiling regimes in the early stages of cooling. The effects of initial temperature, water jet temperature and velocity on the heat transfer coefficient were analyzed by inverse heat conduction method that predicts the heat flux and temperature on the top surface from temperatures measured with thermocouples inserted in test plate. Heat transfer is strongly affected by the initial temperature of the hot steel, water jet temperature and, less intensely, by jet velocity. High cooling rates start when liquid water is in direct contact with surface temperatures above 700°C.The results will contribute to the enhancement of the temperature cooling control on the runout table and cooling model employed at Usiminas Hot Strip Mill.
Keywords: Hot strip mill; Water jet cooling; Heat transfer coefficient; Temperature control.

[1] *Mechanical Engineer, Ph.D., Specialist Researcher, R&D Department, Usiminas Steel, Ipatinga, MG, Brazil.*
[2] *Physicist, Ph.D., Head of Department/Professor, Chair Interfaces with Mass Transfer, Department of Chemical Engineering, Eindhoven University of Technology, Eindhoven, Netherlands.*
[3] *Mechanical Engineer, Dr., Professor, Department of Mechanical Engineering, Federal University of St Catarina, Florianopolis, SC, Brazil.*

1 INTRODUCTION

Many industrial applications use free impinging water jets, because of the high heat transfer rates that can be obtained using relatively simple equipment [1,2]. The temperature control at the runout table is one of the most critical processes to obtain the desired grain structure in a steel strip and ensure required mechanical properties. For a hot strip mill, the finishing and the coiling temperatures are between 800°C-950°C and 510°C-750°C, respectively. In order to reduce the temperature of the strip at the exit of the last stand of the finishing mill to the desired coiling temperature, it is mainly cooled by the cooling water on the runout table. The range of required surface temperatures, heat fluxes and cooling rates are typically very large, which makes it important to obtain an accurate value of the heat transfer coefficient [3,4]. This process includes internal conduction, forced convection, boiling, air convection, radiation and heat generation from material phase transformation. The entire heat transfer process is not yet fully understood because the heat transfer mechanism involves the complex interaction of water impingement and boiling on a moving surface travelling up to 20 m/s [2,5]. The purpose of the present study is to contribute to the understanding of the heat transfer behavior that occurs during the controlled cooling of high-temperature steel by impinging circular water jets. This paper presents an experimental and numerical study of the heat transfer behavior of a high temperature (450°C - 900°C) steel plate cooled by a water jet at 20°C to 70°C. High-speed imaging (up to 20,000 fps) within water jet impingement zone allowed the characterization of the boiling regimes in the early stages of cooling. The effects of jet temperature, jet velocity and initial test temperature on the heat transfer coefficient were analyzed by means of the transient inverse heat conduction method that predicts the heat flux and temperature on the top surface from temperatures measured with thermocouples inserted in test plate.

2 MATERIAL AND METHODS

The main components of the experimental setup are schematized in Figure 1-a. Normal tap-water is stored in an open head tank in which the water temperature is controlled by a thermostat controller. Water is pumped from the collecting reservoir to the head tank. An overflow tube kept the water level in the head tank constant, which ascertains a constant pressure and a stable water jet at the nozzle exit. The water was heated up by an electrical immersion heater and recirculated through head tank, water box and reservoir until the desired temperature was reached everywhere. The inner diameter of nozzle is 9.7 mm and the nozzle is positioned centrally above the test plate surface. The water flow rate is set by a needle valve. A high-speed camera, #2 captures images from the outside of the jet at 300 fps.

The main characteristic that differentiates this test rig from other studies is the ability to optically observe interfacial phenomena through the water jet on the hot surface of the plate allowing the characterization of the boiling regimes in the early stages of cooling. To this end, a borescope is mounted in a box that is fully filled with liquid. The borescope is connected to the high-speed video camera #1 and is positioned centrally above the hole of nozzle exit in a way that does not disturb the water jet stability. In this way, recordings through the water jet yield top views from the jet impingement zone at a rate of 5 to 20 kfps. A series of LED lights surrounding the nozzle exit provide sufficient illumination for this purpose. A cylindrical coordinate system is defined in which r is the radial distance to the center of the jet and y the height above the surface of the plate. Figure 1-b shows the

cross section of a jet of 8 mm impinging on test plate of 50 x 50 x 10 mm³.

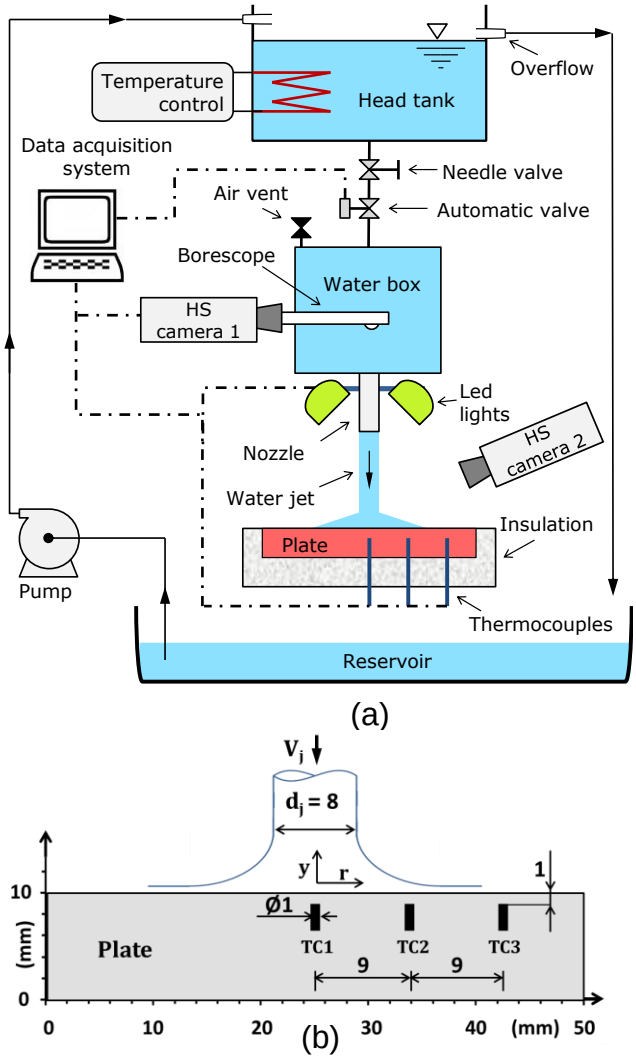

Figure 1. (a) Schematic of the test rig; (b) Schematic of cross section jet impinging on test plate with thermocouples TC1, TC2, and TC3 located in line at radial positions (r).

The impinging jet diameter is similar those used in hot strip mill cooling. The test plate material chosen was the traditional austenitic stainless steel (SS) type 304 for two reasons. First, because its resistance against high temperature oxidation on surface, which is ensured by the formation of protective chromium oxide (Cr_2O_3) film [6]. Second, to avoid the noticeable amount of heat generation, common in carbon steel, caused by phase transformation that distracts temperature reading during jet cooling process. On the plate sides without water impingement, insulation with low thermal conductivity of 0.11 W/(m.K) at 800°C and 25 mm thick was used. Three holes with diameter of 1.1 mm and 9 mm depth were drilled and checked by calipers. Grounded thermocouples Type-K, 1 mm in sheath diameter made of 304 SS (the same as test plate), was used to measure the temperature history. The thermocouples TC1, TC2 and TC3 are located in line at radial positions of 0, 9 and 18 mm, respectively, from the center of plate at depth of 1 mm below the top surface. High temperature thermal paste with conductivity of 70 W/(m.K) was inserted into the hole to insure good thermal thermocouple-plate contact. The thermal properties of the 304 SS [7] are shown in Table 1.

Table 1. Thermophysical properties of the 304 SS.

T (ºC)	c_p (J/kg.K)	ρ (kg/m³)	k (W/m.K)
27	447	7900	15.2
127	515	7859	16.6
327	557	7774	19.8
527	582	7685	22.6
727	611	7582	25.4
927	640	7521	28.0

The test plate was heated by an electrical oven (3 kW) at test quenching position. The data acquisition system simultaneously triggers the automatic valve, the high-speed camera, LED lights and acquires and stores the data. The plate temperature history during cooling process was measured by three thermocouples inserted into the test plate at rate of 50 Hz. The test plate was heated 50°C beyond the initial test temperature. The quenching tests were carried out at T_i of 450°C, 600°C, 750°C, and 900°C which are commonly used in hot strip mill cooling. The water was heated up by electrical heater and recirculated through head tank, water box and reservoir until reach the desire test temperature. The water jet temperatures were 20°C, 50°C and 70°C (subcooling of 80K, 50K and 30K) with velocities of 1 and 3 m/s. Before each experiment, the impinging surface was

sanded with 320 grit sandpaper and cleaned with acetone. The measured arithmetic mean roughness (Ra) at impingement zone surface, after quenching test, was found ranging 0.11 to 0.18 µm. For the new plate surface Ra = 0.10 µm.

Some hydrodynamic parameters are required in a heat transfer analysis of jet impingement quenching, such as impinging jet velocity (V_j), impinging jet diameter (d_j) and active pressure (P_j) at the impingement zone. These parameters at stagnation point (r = 0) are listed in Table 2 and were calculated using the equations of continuity and Bernoulli. The stagnation pressure (P_j) represents the active pressure in the stagnation point (r = 0) at impinging jet velocity (V_j) on plate surface and atmospheric pressure of 101 kPa. In the hot strip mill cooling $V_j \approx 7$ m/s, the saturation temperature (T_{sat}) raises to 105°C.

Table 2. Hydrodynamic parameters at stagnation point (r = 0).

Q_n (ℓ/min)	d_n (mm)	V_n (m/s)	d_j (mm)	V_j (m/s)	P_j (kPa)	T_{sat} (°C)
3	9.7	0.7	8	1	102	100
9	9.7	2.0	8	3	106	101

A widely used commercial inverse heat conduction program INTEMP [8,9,10] was used to predict the heat flux and temperature distribution along the cooling surface from temperature histories measured with thermocouples inserted in the test plate. A 2D axisymmetric finite element model was used for the analysis of the data of the present study. The model had 25 mm in radius, 10 mm thickness with 600 and 1000 quadratic elements of 0.5 x 0.5 and 0.5 x 0.2 mm², respectively, with 4-nodes per element, as showed in Figure 2. The small elements of 0.5 x 0.2 mm² filled the first 4 mm from the top surface with thinner elements in the vertical direction, because of the faster response that is needed close to quenching surface. The faces of the plate without jet impingement were considered adiabatic, since the radiation and free convective heat transfer rate at those surfaces are much less than the one at the impinging side. The impingement surface was divided into three unknown heat flux zones: $r_1 = 0$ to 5 mm (Zone 1); $r_2 = 5$ to 14 mm (Zone 2); $r_3 = 14$ to 25 mm (Zone 3). The measured temperature histories are given as input at the nodes corresponding to the positions of the thermocouples TC1, TC2 and TC3 located at 1 mm from top surface at radial position of r = 0, 9, and 18 mm, respectively. Details of this model and validation are described in [11].

Calculated uncertainty was within 95% limits and was analyzed according to criteria suggested by Taylor [12] taking into account errors in measurement, calibration, machining, and measuring devices. Combining the uncertainties of thermocouple and data acquisition system, the uncertainty of temperature was ± 0.30%. The calculated relative uncertainty for heat flux (q) was ± 5 %.

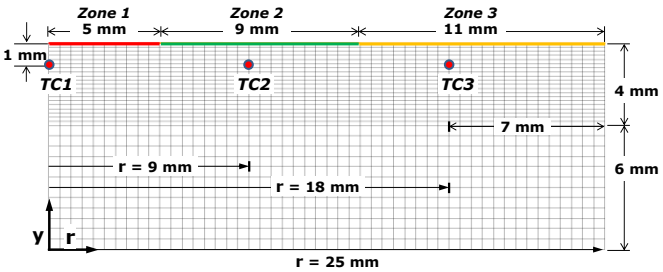

Figure 2. 2D axisymmetric finite element model divided into three unknown heat flux monitoring zones on top plate surface.

3 RESULTS AND DISCUSSION

A sequence of snapshots of the jet cooling experiment for $T_i = 896$°C and $T_j = 20$°C, showing the growth of the wetted region, is shown in Figure 3. The plate surface initially at 896°C (t = 0) becomes covered by insulating vapor blanket after the jet has impinged on its surface (t = 0.06 s). A small darker zone is formed at t = 0.27 s under the jet indicating that the solid-liquid contact (rewetting) was established. Rewetting temperature (T_{rw}) is defined as

the surface temperature that allows the establishment of the direct contact of a liquid with a hot surface. Rewetting delay time (t_{rw}) is the time to rewetting occurs after jet has impinged on hot surface.
Within wetted region the regime changes from film to nucleate boiling. Outside this small region, the surface is dry and a vapor blanket occurs. The wetted region grows fast moving radially outward (t = 0.38 s). A white narrow band demarcates the frontier between wetted and dry zone (rewetting front). The free-surface on top of the liquid flow appears smooth and shiny, without visible evidence of boiling activity within the wetted region (t = 0.44 s).

Figure 3. Sequence of events of the wetted region growth for T_i = 896°C and T_j = 20°C.

Even though this visible absence of bubbles was reported by Leocadio et al. [3], top view images from within the jet impingement zone with vigorous boiling activity will be showed in the present study. Outside of the wetted region, the outgoing water is deflected upward. The rewetting front velocity, V_{rw}, decreases as the wetted zone grows radially outwards. The wetted zone diameter enlarges from t = 0.38 s to 0.68 s (0.3 s) a radial advance of 14 mm and after long period of 1.52 s (t = 2.20 s) a radial advance only of 1 mm. This sudden drop in rewetting velocity is explained from the heating and thinning of the water film while it moves radially outwards: it loses its ability to condense vapor at rewetting front edge, this analysis is in line with Karwa et al. [13] and Lee et al. [14].
Figure 4 shows boiling regimes and cooling and curves for T_i = 751°C, T_j = 20°C, and V_j = 1 m/s. Figure 4-a shows top view images inside of water jet impingement (from A to H) of successive stages of boiling regimes which are indicated on curves seen in Figure 4 (b) which depicts the boiling regimes (film boiling, transition, maximum heat flux, nucleate boiling, and single-phase) by cooling curve, heat flux, cooling rate, and heat transfer coefficient during the quench test.
Film boiling still cover the hot surface 0.02 s after quenching has started (Stage A) and the surface temperature (T_s) remain unaltered due to the low heat transfer across vapor layer where heat flux, heat transfer coefficient, and cooling rate are low. The red dashed circles show some of many gas bubbles on vapor film. Such gas bubbles are coming from a degassing process explained by Leocadio et al. [11].
At t_{rw} = 0.11 s (Stage B) the establishment of the direct steel-liquid contact (rewetting) occurs on very high-temperature steel surface at 738°C and surface heat flux (q) is only 1.1 MW/m². Two small wetted regions can be seen within the red dashed circle, and vapor film still exists surrounding this region.

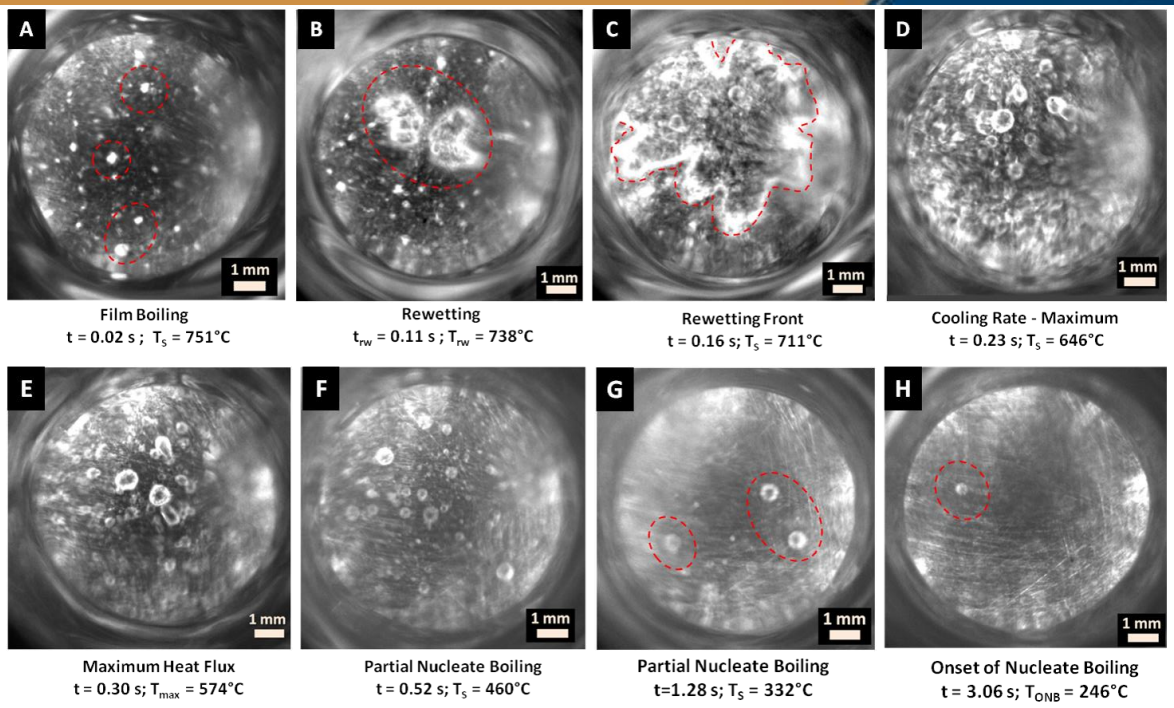

(a) Snapshots of successive stages of boiling regimes within jet impingement zone.

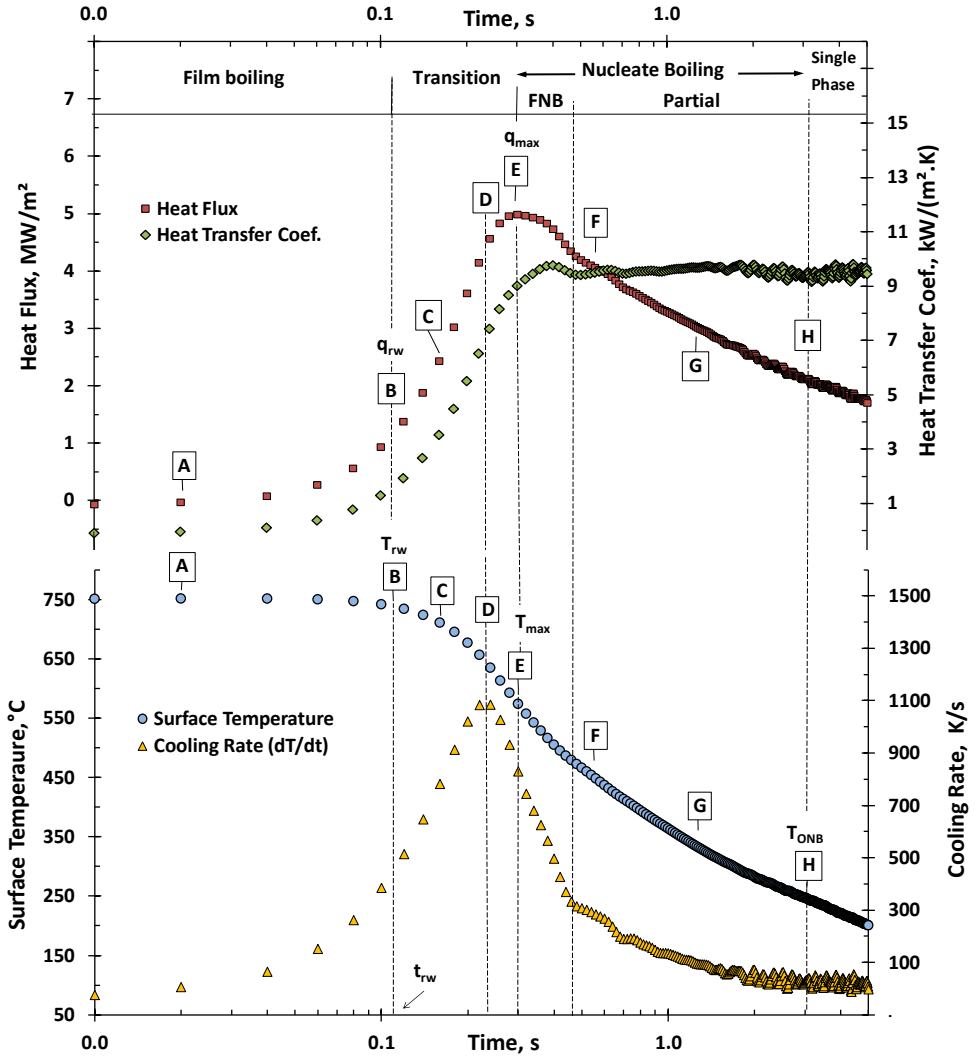

(b) Cooling curve, heat flux, cooling rate, and heat transfer coefficient.

Figure 4. Heat transfer and boiling regimes in jet impingement quenching for T_i = 751°C, T_j = 20°C.

The rewetting phenomenon occurring on high-temperature surface beyond critical point of water (374°C) is explained by Leocadio et al. [11]. They proposed equations (1) and (2) for the prediction of the rewetting temperature (T_{rw}) and rewetting delay time (t_{rw}), respectively.

$$\mathbf{T_i - T_{rw} = \frac{22563}{\Delta T_{sub}^{1.44}\, V_j^{0.092}} \left(\frac{T_i - 450}{450 - T_{sat}}\right)^3} \quad (1)$$

$$\mathbf{t_{rw} = 0.00153 \exp\left[\frac{T_i\,(37 - 1.92\,V_j)}{1000\,\Delta T_{sub}^{0.421}}\right]} \quad (2)$$

where $\Delta T_{sub} = T_s - T_{sat}$ is the water jet subcooling. The wetted area (nucleate boiling regime) increases over time due to the advancement of rewetting front outwards in radial direction (red dashed line), where many vapor bubbles are observed, while out of this area the gas bubbles still remain on film boiling (dry area). In Stage C, the surface temperature (T_s) dropped to 711°C, while heat flux (q_s) increased to 2.4 MW/m². At Stage D the surface is fully wetted and only vapor bubbles are observed and the cooling rate (CR) is maximum (1083 K/s) at t = 0.23 s with T_s = 646°C, and q_s = 4.4 MW/m². At Stage E, the maximum heat flux (q_{max}) of 5.0 MW/m² occurs at t = 0.30 s, T_s = 574°C, and CR = 830 K/s.

After the peak of maximum heat flux (Stage E) the direction of the heat flux curve changes downward. The heat transfer coefficient (h) reaches its maximum value (≈ 9.5 kW/m².K) between Stages E and F and remains almost constant going through single-phase regime. The curve shows heat transfer coefficient in film boiling regime is very low, increasing during in transition regime.

The snapshots at Stage E - F clearly show the gradual reduction in bubble population due to the surface temperature reduction of 574°C to 332°C. The bubbles size seemed non-change over time with the surface temperature reduction, what shows the independence of bubble size from surface temperature.

Over time the cooling process continues until the surface temperature reaches the value of 246°C, where bubbly activity ceases and just a bubble is observed (Stage H). The bubbly activity has ceased due to high subcooling of water. Increasing water jet temperature was observed a increasing in bubbles size and a decreasing on surface temperature to cease the bubbly activity. Figure 5 shows the effect of initial surface temperature (T_i) on the heat flux curve for jet temperature (T_j) of 20°C, r = 0, and V_j = 1 m/s. Maximum heat flux (q_{max}) increases with the rise the initial surface temperature. For T_i = 450°C, 600°C, 750°C and 900°C, q_{max} = 2.6, 3.3, 5.1, 6.4 MW/m² occurs at T_s = 393°C, 453°C, 578°C and 653°C, respectively. This demonstrates the strong influence of initial surface temperature on q_{max}.

Note that, this inflection on curves indicates probably defines the onset of single-phase about the surface temperature of 250°C, as shown in image of Stage H in Figure 4-a. In single-phase regime all curves remain together, regardless of T_i. Due to the end of bubbly activity, the heat transfer happens by forced convection and it depends on only liquid flow. Therefore, Maximum heat flux and nucleate boiling regime strongly depend on T_i, while it has a weak influence on single-phase regime.

Figure 6 shows the effect of T_i on heat transfer coefficient at r = 0, for V_j = 1 m/s, jet of 20°C, and T_i = 450°C, 600°C, 750°C and 900°C.

At the beginning of cooling process the heat transfer coefficient (h) value is too low for all T_i but they increases as surface temperature (T_s) reduces up to maximum heat transfer coefficient (h_{max}) is achieved. For T_i = 450°C and 900°C, h_{max} = 7 and 13.5 kW/m².K, respectively.

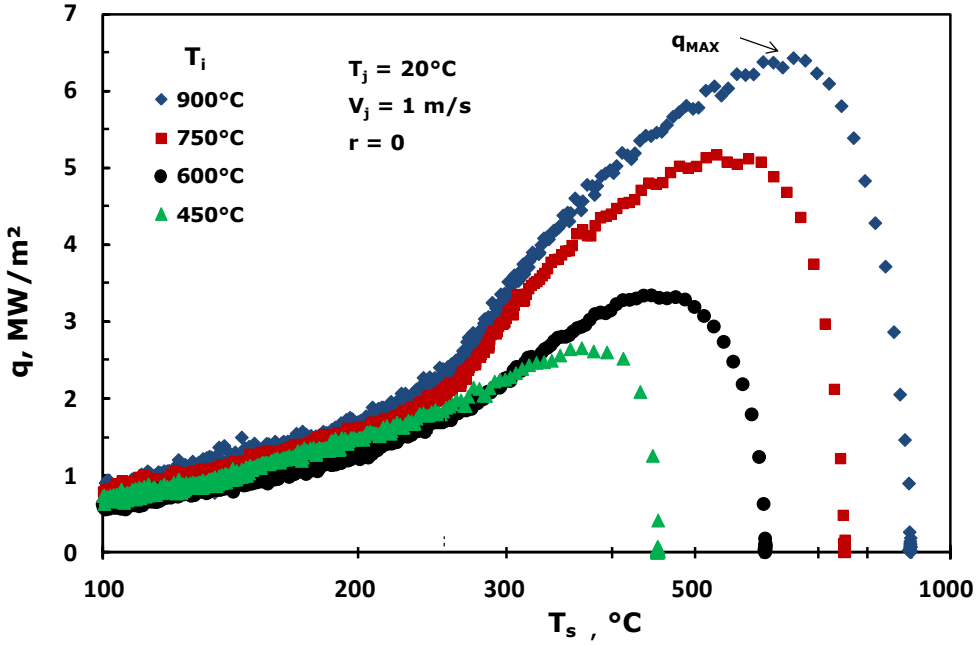

Figure 5. Effect of initial surface temperature on the boiling curve for jet temperature of 20°C and r = 0.

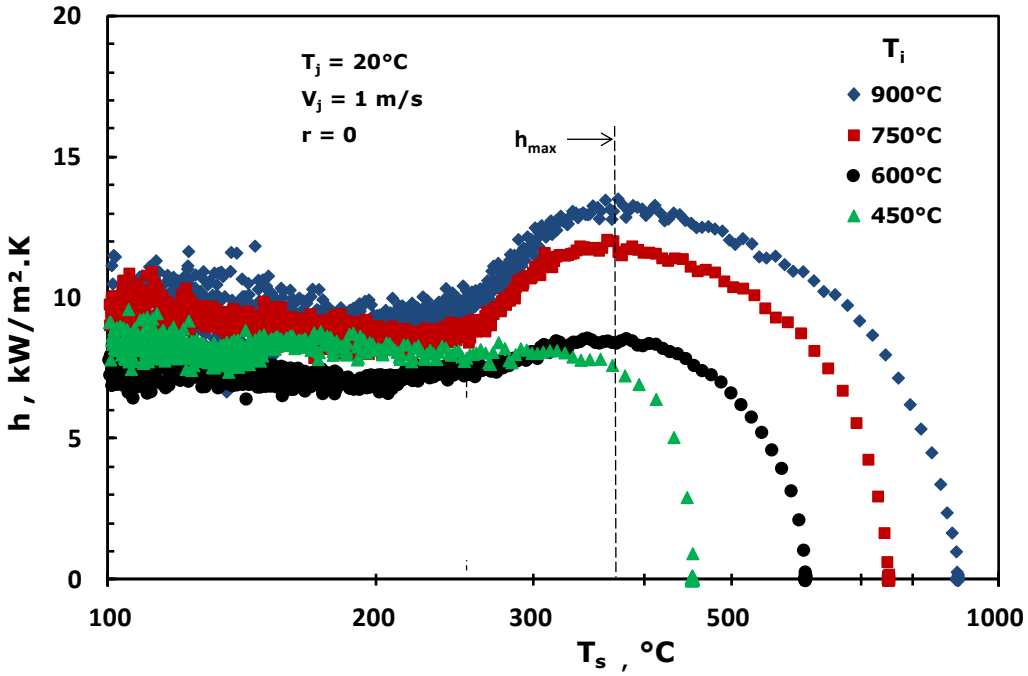

Figure 6. Effect of T_i on heat transfer coefficient at r = 0, for V_j = 1 m/s and jet temperature of 20°C.

It was observed a trend in h_{max} to occur on surface temperature at 350°C – 400°C, independently of T_i. However, after h_{max}, all curves go to downward direction and remain relatively constant after surface temperature about 250°C with $h \approx 6$ and 11 kW/m².K, for T_i = 450°C and 900°C, respectively. As above explained, this inflection on curves indicates probably the onset of single-phase. This could be the explanation for the h curves remain constant on this region. Therefore, heat transfer coefficient is strongly affected by T_i and T_s.

The heat transfer coefficient curves, at right side of h_{max}, should be used as boundary condition in controlled cooling models for hot rolling mill line, because the

common range of surface temperature is $350°C < T_s < 900°C$. Constant values of heat transfer coefficient have to be avoided in such models.

Figure 7 shows the effect of initial temperature (T_i) on radial distribution of surface heat flux, for $T_j = 20°C$ and $V_j = 1$ m/s at (a) $T_i = 450°C$, (b) $T_i = 750°C$, (c) $T_i = 900°C$. The delay time between peaks of maximum heat fluxes is caused by delay in the rewetting front arrival (growth of wetted zone), as showed in Figure 3. The time lapse among peaks of maximum heat fluxes for $T_i = 450°C$ (Figure 7 - a) are smaller than for $T_i = 900°C$. Larger initial surface temperature increases the amount of energy stored in the test plate, thereby increasing the time needed to extract energy and, thus, reducing the rewetting front propagation. As the test plate has more energy stored when T_i is higher, thus it has more energy to be delivery what leads to higher values in heat fluxes in $T_i = 900°C$ and lower values in $T_i = 450°C$. Note as the heat flux curves were shifted up in Figure 7 - c.

Therefore, heat flux curves are strongly affected by T_i. The delay time among maximum heat fluxes are enlarged with increasing of T_i, because higher T_i reduce the ability of water to condense vapor at rewetting front edge, thus, the growth velocity of the wetted zone. This behavior also was observed in others studies [3,13].

The experiment for the effect of jet impinging velocity (V_j) on radial distribution of surface heat flux, for $T_i = 900°C$ and $T_i = 20°C$ at $V_j = 1$ m/s and 3 m/s demonstrated that the lapse of time among peaks of q_{max} was smaller for $V_j = 3$ m/s than 1 m/s. The explanation for this is the larger mass of water on surface for $V_j = 3$ m/s resulting in a smaller heating of water increasing the ability of condensing and removing bubbles at rewetting front, consequently, increasing the rewetting front velocity and reducing the time lapse among peaks.

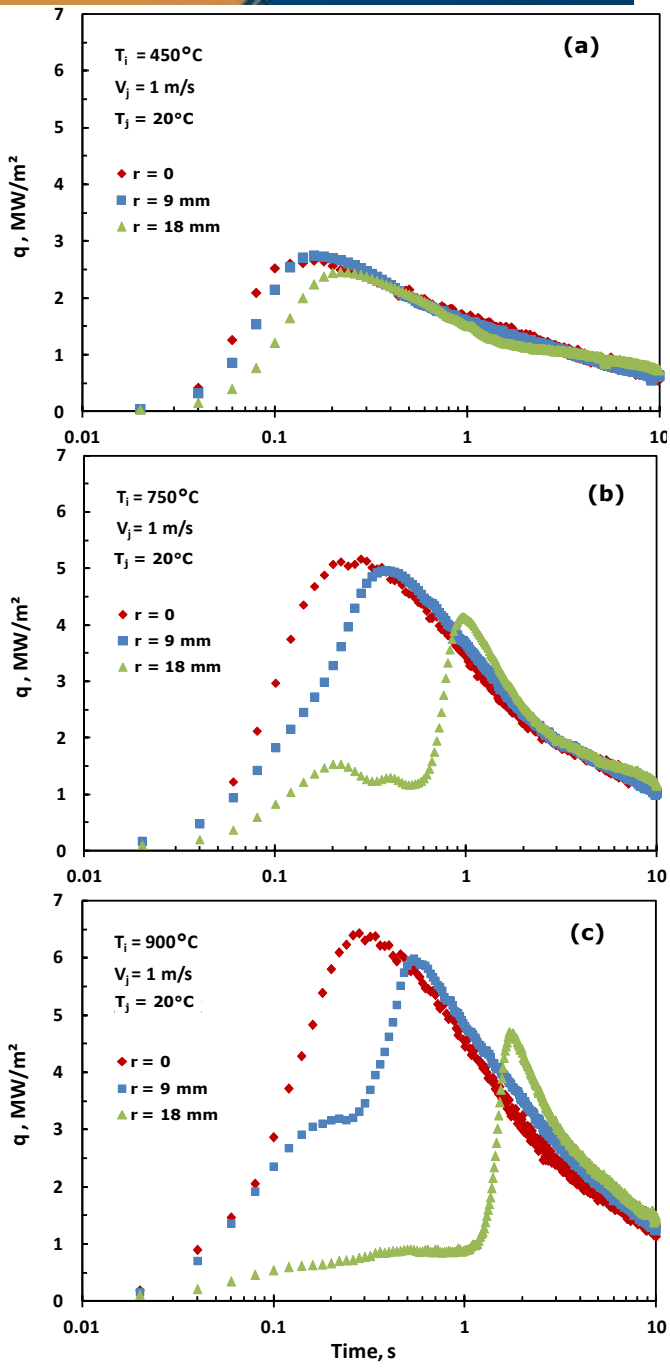

Figure 7. Effect of initial surface temperature on radial distribution of surface heat flux, for $T_j = 20°C$ and $V_j = 1$ m/s at (a) $T_i = 450°C$, (b) $T_i = 750°C$, (c) $T_i = 900°C$.

However, the same experiment demonstrated the weak effect of jet velocity on heat flux curve, with $V_j = 1$ m/s and 3 m/s. Increasing V_j lightly increases the heat flux. The experiment for the effect of subcooling on radial distribution of surface heat flux for $T_j = 20°C$, 50°C, and 70°C demonstrated that subcooling has a strong effect on heat flux curve and rewetting front

velocity. Increase in subcooling increase both rewetting front velocity and value of heat flux on radial distribution, and reduce the lapse of time to occurrence of q_{max}. This experiment also demonstrated the strong effect of subcooling on heat flux curve. Decreasing the jet temperature has an increasing in the heat flux.

4 CONCLUSION

The characterization of the heat transfer during the cooling of a high temperature steel plate by an impinging water jet was successfully performed using an experimental apparatus with the aid of a novel high speed imaging technique and main findings were:

Surface heat flux is strongly affected by water jet temperature and surface temperature, and weakly by jet velocity. Higher surface temperature and lower jet temperature increase surface heat flux.

Heat transfer coefficient is strongly affected by surface temperature. Increasing initial surface temperature increases the heat transfer coefficient. Constant values of heat transfer coefficient have to be avoided in controlled cooling models for hot rolling mill line, because it intensely varies with cooling surface temperature in the range of $350°C < T_s < 900°C$.

Wetted zone increases faster for lower initial surface temperatures and lower water jet temperatures. Since, within wetted zone the heat flux is about 5 times larger than dry zone, variable wetted area must be used in accelerated cooling models for hot rolling mill.

REFERENCES

1 Agrawal, C, Kumar, R and Gupta, A Rewetting and maximum surface heat flux during quenching of hot surface by round water jet impingement. International Journal of Heat and Mass Transfer. 2012, Vol. 55, pp. 4772-4782.

2 Lee, P, Choi, H and Lee, S, The Effect of Nozzle Height on Cooling Heat Transfer from a Hot Steel Plate by an Impinging Liquid Jet. Iron and Steel Institute of Japan International. 2004, Vol. 44, 4, pp. 704-709.

3 Leocadio, H, Passos, JC and Silva, AFC, Heat transfer behavior of a high temperature steel plate cooled by a subcooled impinging circular water jet, in 7th ECI International Conference on Boiling Heat Transfer, 2009.

4 Filipovic, J, Incropera, FP and Viskanta, R, Rewetting temperature and velocity in a quenching experiment. Experimental Heat Transfer. 1995, Vol. 8, 4, pp. 257-270.

5 Nobari, AH, Prodanovic, Vand Militzer, M, Heat transfer of a stationary steel plate during water jet impingement cooling. International Journal of Heat and Mass Transfer, 2016, Vol. 101, pp. 1138-1150.

6 Sabioni, ACS, et al., About the role of chromium and oxygen ion diffusion on the growth mechanism of oxidation films of the AISI 304 austenitic stainless steel, Oxidation of Metals, 78, pp. 211-220, 2012.

7 Incropera, FP, et al., Fundamentals of Heat and Mass Transfer. 7th: John Wiley & Sons, 2011.

8 Ravikumar, SV, Jha, J Mand Tiara, AM, Experimental investigation of air-atomized spray with aqueous polymer additive for high heat flux applications. International Journal of Heat and Mass Transfer, 72, pp. 362-377. 2014.

9 Trujillo, DM and Busby, HR, Practical Inverse Analysis in Engineering. Boca Raton: CRC Press, 1997.

10 Leocadio, H, Interfaces and heat transfer in jet impingement on a high temperature surface, PhD thesis, Eindhoven University of Technology, 2018.

11 Leocadio, H, Van der Geld, CWM and Passos, JC. Rewetting and boiling in jet impingement on high temperature steel surface, Physics of Fluids, 12, 2018, Vol. 30, p. 122102.

12 Taylor, JR, An Introduction to Error Analysis - The Study of uncertainties in physical measurements. Second Edition: University of Colorado, 1996.

13 Karwa, N and Stephan, P, Experimental investigation of free-surface jet impingement quenching process. International Journal of Heat and Mass Transfer. 2013, Vol. 64, pp. 1118-1126.

14 Lee, SG, et al., Quasi-steady front in quench subcooled-jet impingement boiling: Experiment and analysis. International Journal of Heat and Mass Transfer. 2017, Vol. 113, pp. 622-634.